

# Structural Variations in Tetrasilver(I) Complexes of Pyrazolate-bridged Compartmental *N*-Heterocyclic Carbene Ligands

Maria Georgiou, Simone Wöckel, Vera Konstanzer, Sebastian Dechert, Michael John, and Franc Meyer

Institut für Anorganische Chemie, Georg-August-Universität Göttingen, Tammannstraße 4, 37077 Göttingen, Germany

Reprint requests to Prof. Dr. Franc Meyer. Fax: +49551393063.

E-mail: franc.meyer@chemie.uni-goettingen.de

*Z. Naturforsch.* **2009**, *64b*, 1542–1552; received October 13, 2009

*Dedicated to Professor Hubert Schmidbaur on the occasion of his 75<sup>th</sup> birthday*

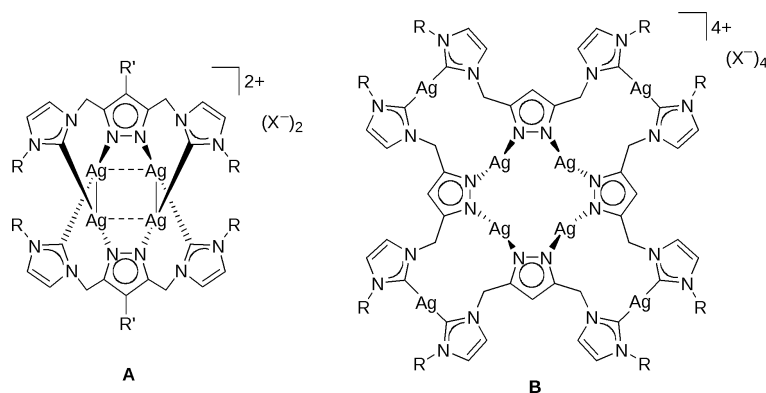
A set of pyrazole-bridged bis(imidazolium) compounds  $[\text{H}_3\text{L}^1]\text{X}_2 - [\text{H}_3\text{L}^4]\text{X}_2$  ( $\text{L}^1 = 3,5\text{-bis}[1\text{-}(tert\text{-butyl})\text{imidazolium-1-ylmethyl}]\text{-}1H\text{-pyrazole}$ ;  $\text{L}^2 = 3,5\text{-bis}[1\text{-}(tert\text{-butyl})\text{imidazolium-1-ylmethyl}]\text{-}4\text{-phenyl-}1H\text{-pyrazole}$ ;  $\text{L}^3 = 3,5\text{-bis}[1\text{-}(1\text{-adamantyl})\text{imidazolium-1-ylmethyl}]\text{-}1H\text{-pyrazole}$ ;  $\text{L}^4 = 3,5\text{-bis}[1\text{-}(1\text{-adamantyl})\text{imidazolium-1-ylmethyl}]\text{-}4\text{-phenyl-}1H\text{-pyrazole}$ ;  $\text{X} = \text{Cl}^-$ ,  $\text{BF}_4^-$  or  $\text{PF}_6^-$ ) has been prepared, and three compounds have been characterized by X-ray crystallography. The unique  $[\text{H}_3\text{L}^4][\text{H}_2\text{L}^4](\text{PF}_6)_3$  features a dimeric face-to-face arrangement of two molecules due to the involvement of both the pyrazole-NH and the imidazolium  $\text{C}^2\text{H}$  in hydrogen bonding.  $[\text{H}_3\text{L}^1]\text{X}_2 - [\text{H}_3\text{L}^4]\text{X}_2$  serve as precursors for silver(I) complexes with compartmental pyrazolate-bridged bis(NHC) ligands. The complexes have been readily prepared by the  $\text{Ag}_2\text{O}$  route and feature either the known  $[(\text{L}^{1-4})_2\text{Ag}_4]^{2+}$  or the new  $[(\text{H}_2\text{L}^1)_4\text{Ag}_4]^{8+}$  motif, depending on the solvent for the reaction (MeCN or acetone).  $[(\text{H}_2\text{L}^1)_4\text{Ag}_4](\text{PF}_6)_8$  contains a central  $(\text{pzAg})_4$  ring with pendant imidazolium side arms. Upon further reaction with  $\text{Ag}_2\text{O}$  in MeCN it was found to undergo transformation to the corresponding  $[(\text{L}^1)_2\text{Ag}_4](\text{PF}_6)_2$ . All complexes have been thoroughly studied by NMR spectroscopy in solution, and preliminary luminescence data of  $[(\text{H}_2\text{L}^1)_4\text{Ag}_4](\text{PF}_6)_8$  have been recorded.

*Key words:* *N*-Heterocyclic Carbenes (NHC), Pyrazole, Silver, Oligonuclear Complexes

## Introduction

*N*-Heterocyclic carbenes (NHCs) are currently ranking among the most popular ligands in organometallic chemistry [1]. A convenient and widely applied method for the preparation of various metal-NHCs is the transmetallation of Ag(I)-NHC complexes, since Ag(I)-NHCs are readily available *via* the so called “ $\text{Ag}_2\text{O}$  route” [2]. This involves the *in situ* deprotonation of an imidazolium ligand precursor by a basic silver(I) salt, usually  $\text{Ag}_2\text{O}$ , without the need of strictly anaerobic conditions or any pre-treatment. Numerous publications have appeared during the last decade that make use of this method, and because of their easy preparation and their synthetic value, a multitude of Ag(I)-NHC complexes have been studied; an overview is available from several recent reviews [3–5]. Apart from their use as carbene transfer agents, Ag(I)-NHC complexes

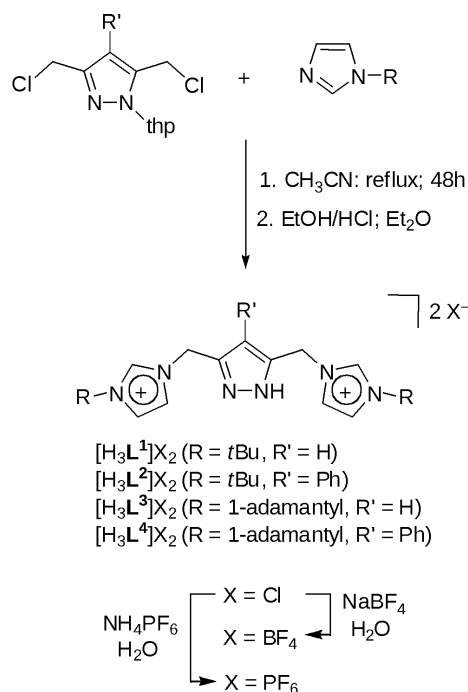
are highly interesting themselves and offer potential applications as, *inter alia*, luminescence materials or precursors for Ag nanoparticles. A large variety of structural motifs in Ag-NHC chemistry can be realized by variation of the reaction conditions or the employed anions and by alteration of steric and electronic properties of the NHC ligands. The scope is further extended by introducing functional donor substituents to the NHC or combining several NHC moieties in multidentate chelate scaffolds [6]. Some groups including ours have recently reported pyrazole-bridged bis(NHC) ligands [7–9] that provide two proximate binding compartments and give rise to unique multinuclear Ag(I)-NHC complexes [9, 10]. Compounds  $[\text{LAg}_2]_n$  with two very different structures have been observed: a planar  $\text{Ag}_4$  core sandwiched between two pyrazolate/NHC ligands (**A**;  $n = 2$ ) [9, 10] or an unprecedented  $\text{Ag}_8$  double metallocrown (**B**;  $n = 4$ ) [10].



Complex **B** features an inner metallocrown with homoleptic N(pyrazolate) coordination and a surrounding outer metallocrown with homoleptic bis(NHC) coordination of the metal ions. This represents two of the well-known structural themes in silver(I) coordination chemistry, namely linear  $[\text{Ag}(\text{NHC})_2]^+$  and cyclic  $[\text{M}(\mu\text{-pz})_n]$ ; such  $[\text{M}(\mu\text{-pz})_n]$  rings are commonly found in coinage metal pyrazolate complexes (mostly with  $n = 3$ ) [11]. This raises interesting questions concerning the relation and possible competition between these two binding motifs. It was speculated that the formation of different structures **A** and **B** despite similar ligand scaffolds and identical metal : ligand ratio (2 : 1 or 4 : 2) in the Ag(I)-pyrazolate/NHC systems might be caused by the different steric bulkiness of the NHC substituents [5, 10]. In the present contribution we thus describe the synthesis of several new compartmental pyrazolate/NHC ligands with very bulky imidazolium substituents (*tert*-butyl, 1-adamantyl), we introduce different substituents at the pyrazolate- $\text{C}^4$  backbone (H, Ph), and we explore the Ag(I) coordination chemistry of the new set of ligand scaffolds. Most interestingly, the structural landscape of these systems seems to be even more complicated, as a new complex with an Ag : ligand ratio of 4 : 4 could be isolated and structurally characterized.

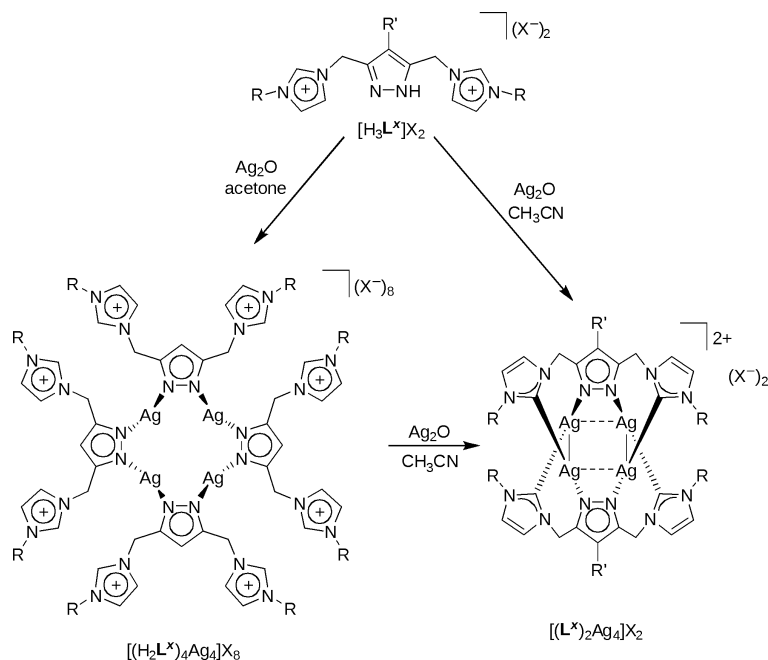
## Results and Discussion

The hygroscopic bis(imidazolium) chlorides  $[\text{H}_3\text{L}^1]\text{Cl}_3 - [\text{H}_3\text{L}^4]\text{Cl}_3$  were prepared from 3,5-bis(chloromethyl)-1-(tetrahydropyranyl-2-yl)-4-phenyl-1*H*-pyrazole and the respective *N*-substituted imidazole in close analogy to the procedure reported previously (Scheme 1) [8, 10]. Subsequent treatment of aqueous solutions of the chloride salts with an



Scheme 1. Synthesis of ligand precursors  $[\text{H}_3\text{L}^1]\text{X}_2 - [\text{H}_3\text{L}^4]\text{X}_2$ . thp = tetrahydropyran-2-yl.

excess of  $\text{NH}_4\text{PF}_6$  or  $\text{NaBF}_4$  allowed the isolation of the corresponding hexafluorophosphate and tetrafluoroborate salts, respectively (Scheme 1). The latter are preferred ligand precursors because of their increased solubility compared to the chloride salts. All four new pyrazolate-bridged bis(imidazolium) compounds, which differ by the imidazolium substituent  $\text{R}$  (*t*Bu or 1-adamantyl) and the backbone substituent at the pyrazole- $\text{C}^4$  ( $\text{R}' = \text{H}$  or Ph), were characterized by elemental analysis, mass spectrometry and NMR spectroscopy.



Scheme 2. Synthesis of silver complexes.

When dissolved in  $[\text{D}_6]\text{DMSO}$ , the compounds  $[\text{H}_3\text{L}^{\text{X}}](\text{PF}_6)_2$  and  $[\text{H}_3\text{L}^{\text{X}}](\text{BF}_4)_2$  show one or two (depending on the pyrazole-NH tautomerism) characteristic  $^1\text{H}$  NMR signals between 9.0 and 9.5 ppm, which stem from the acidic imidazolium CH proton ( $\text{CH}^{\text{im}2}$ ). The bridging  $\text{CH}_2$  groups appear as singlets at about 5.4 ppm, while the pyrazole NH proton appears as broad resonance at about 13.3 ppm.  $^1\text{H}$  and  $^{13}\text{C}$  NMR spectra of the imidazolium salts are independent of the counterion ( $\text{BF}_4^-$  vs.  $\text{PF}_6^-$ ).

The constitution of  $[\text{H}_3\text{L}^1](\text{BF}_4)_2$ ,  $[\text{H}_3\text{L}^3](\text{BF}_4)_2$ , and  $[\text{H}_3\text{L}^4](\text{PF}_6)_2$  has been confirmed by X-ray crystallography; the molecular structures are depicted in Figs. S1, S2, and S3, respectively (Supporting Information available online; see paragraph at the end of the paper). In all these compounds, rather close contacts are found between the imidazolium- $\text{C}^2\text{H}$  and/or pyrazole protons and the counteranions. Disorder of the pyrazole moiety and the  $\text{BF}_4^-$  anions in  $[\text{H}_3\text{L}^1](\text{BF}_4)_2$  and  $[\text{H}_3\text{L}^3](\text{BF}_4)_2$ , however, does not allow a detailed discussion of this structural feature. The crystal of  $[\text{H}_3\text{L}^4](\text{PF}_6)_2$  in fact has to be formulated as  $[\text{H}_3\text{L}^4][\text{H}_2\text{L}^4](\text{PF}_6)_3$  since it consists of two types of molecules, one of which is deprotonated at the pyrazole nitrogen atom. Hydrogen bonding between the protonated ( $[\text{H}_3\text{L}^4]^{2+}$ ) and singly deprotonated forms ( $[\text{H}_2\text{L}^4]^+$ ) of the ligand is present, giving rise to a displaced face-to-face arrangement of the two ligand

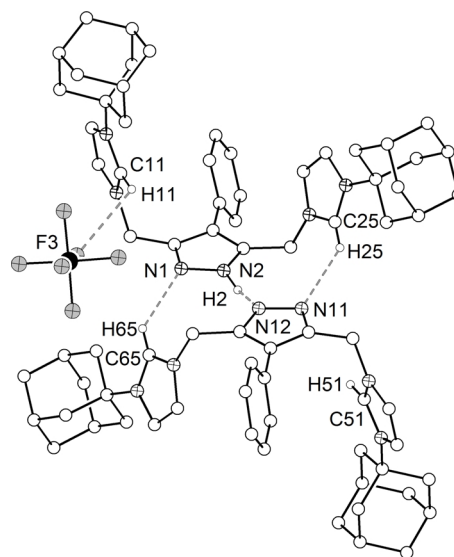


Fig. 1. Plot of the molecular structure of  $[\text{H}_3\text{L}^4][\text{H}_2\text{L}^4](\text{PF}_6)_3$  emphasizing the hydrogen bonding interactions. Selected parameters for hydrogen bonding or close contacts (Å; deg):  $\text{N}2 \cdots \text{N}12$  2.636(3),  $\text{C}11 \cdots \text{F}3$  3.182(4),  $\text{C}25 \cdots \text{N}11$  3.256(4),  $\text{C}65 \cdots \text{N}1$  3.197(4),  $\text{N}2\text{-H}2 \cdots \text{N}12$  155(5),  $\text{C}11\text{-H}11 \cdots \text{F}3$  107(4),  $\text{C}25\text{-H}25 \cdots \text{N}11$  140(5),  $\text{C}65\text{-H}65 \cdots \text{N}1$  137(5).

strands with a central  $\text{N-H} \cdots \text{N}$  and two flanking  $\text{C}^2\text{-H} \cdots \text{N}$  interactions (Fig. 1). Involvement of the imidazolium- $\text{C}^2$  hydrogen atoms in hydrogen bonding

Table 1. Selected bond lengths (Å) and angles (deg) for  $[(L^1)_2Ag_4](BF_4)_2$ ,  $[(L^3)_2Ag_4](BF_4)_2$  and  $[(L^4)_2Ag_4](PF_6)_2$  and  $[(H_2L^1)_4Ag_4](PF_6)_8$  with estimated standard deviations in parentheses.

Distances	$[(L^1)_2Ag_4](BF_4)_2$	$[(L^3)_2Ag_4](BF_4)_2$	$[(L^4)_2Ag_4](PF_6)_2$	$[(H_2L^1)_4Ag_4](PF_6)_8$
Ag1–N	2.097(5)	2.096(3)	2.089(2)	2.070(2) / 2.073(2)
Ag2–N	2.091(4)	2.092(3)	2.097(2)	–
Ag1–C	2.078(5)	2.086(4)	2.073(2)	–
Ag2–C	2.079(6)	2.077(4)	2.077(2)	–
Ag1 ... Ag2 <sup>a</sup>	3.1943(6)	3.2658(4)	3.2955(2)	3.1140(3)
Ag1 ... Ag2'	3.4120(7)	3.3397(5)	3.3840(2)	–
Angles				
Ag1 ... Ag2 ... Ag1' <sup>a,b</sup>	89.5(1)	91.7(1)	89.1(1)	89.9(1)
Ag2 ... Ag1 ... Ag2'	90.5(1)	88.3(1)	90.9(1)	–
C–Ag1–N <sup>c</sup>	178.2(2)	176.6(2)	177.6(1)	167.9(1)
C–Ag2–N	178.0(2)	177.7(2)	175.8(1)	–
N–C–N	105.5(5) / 104.4(5)	104.7(3) / 105.3(3)	104.9(2) / 104.8(2)	108.6(3) / 109.0(3)

<sup>a</sup> Ag2 = Ag1' in  $[(H_2L^1)_4Ag_4](PF_6)_2$ ; <sup>b</sup> Ag1' = Ag1''' in  $[(H_2L^1)_4Ag_4](PF_6)_2$ ; <sup>c</sup> C = N in  $[(H_2L^1)_4Ag_4](PF_6)_8$ .

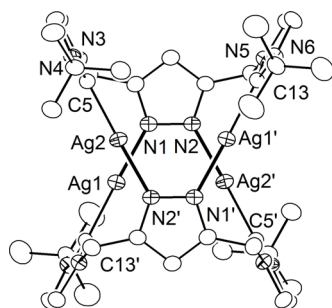


Fig. 2. ORTEP plot (30% probability displacement ellipsoids) of the molecular structure of  $[(L^1)_2Ag_4](BF_4)_2$ . For the sake of clarity all hydrogen atoms, the solvent molecules, and  $BF_4^-$  have been omitted. Symmetry transformation used to generate equivalent atoms: (')  $1-x, 1-y, 1-z$ .

towards a pyrazole-N is unusual, as pyrazoles commonly aggregate *via* N–H ... N hydrogen bonds [12]. One of the remaining peripheral imidazolium-C<sup>2</sup> hydrogen atoms points towards a  $PF_6^-$  anion, with a C(H) ... F distance in the range previously reported for this kind of weak interaction [13].

Reaction of  $[H_3L^x](PF_6)_2$  or  $[H_3L^x](BF_4)_2$  with  $Ag_2O$  in MeCN solutions yielded tetranuclear silver(I)-NHC complexes  $[(L^x)_2Ag_4]^{2+}$  in all cases (Scheme 2). The procedure is simple, and unreacted  $Ag_2O$  can be easily removed by filtration. Unfortunately, however, isolated yields of the products were moderate at best. Better yields (up to 64%, depending on the R and R' substituents) are obtained by the *in situ* salt metathesis method described in the literature [14]. Crystalline material could be obtained for  $[(L^1)_2Ag_4](BF_4)_2$ ,  $[(L^3)_2Ag_4](BF_4)_2$  and  $[(L^4)_2Ag_4](PF_6)_2$ , and molecular structures were determined by X-ray diffractometry (Figs. 2–4).

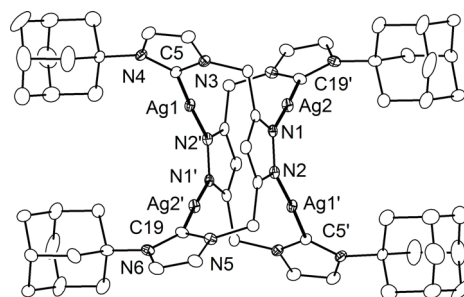


Fig. 3. ORTEP plot (30% probability displacement ellipsoids) of the molecular structure of  $[(L^3)_2Ag_4](BF_4)_2$ . For the sake of clarity all hydrogen atoms, the solvent molecules, and  $BF_4^-$  have been omitted. Symmetry transformation used to generate equivalent atoms: (')  $1-x, 1-y, 1-z$ .

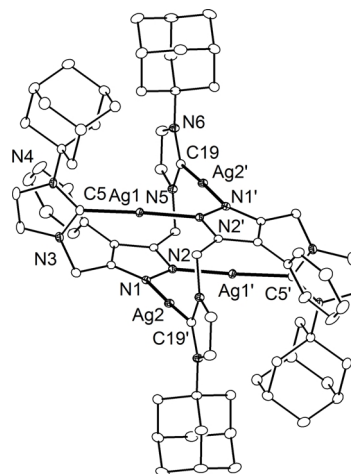


Fig. 4. ORTEP plot (30% probability displacement ellipsoids) of the molecular structure of  $[(L^4)_2Ag_4](PF_6)_2$ . For the sake of clarity all hydrogen atoms, the solvent molecules, and  $PF_6^-$  have been omitted. Symmetry transformation used to generate equivalent atoms: (')  $1-x, 1-y, 1-z$ .

$[(\mathbf{L}^1)_2\text{Ag}_4]^{2+}$ ,  $[(\mathbf{L}^3)_2\text{Ag}_4]^{2+}$  and  $[(\mathbf{L}^4)_2\text{Ag}_4]^{2+}$  represent the common structural motif that has been observed for silver complexes with related ligands combining NHC and pyrazole moieties [9, 10]. However, not more than a handful of complexes of this type have been structurally characterized to date, and the present work confirms that these tetrametallic arrays are formed also in the case of bulky imidazole substituents such as *tert*-butyl or 1-adamantyl. Crystallographically imposed  $C_i$  symmetry is found in all three complexes, each of which consists of four silver atoms and two ligands. The remaining positive charge is compensated either by  $\text{BF}_4^-$  or  $\text{PF}_6^-$  anions. The arrangement of the silver atoms is almost rectangular. Numerous examples for weak metal-metal interactions in  $d^{10}$  coinage metal complexes have been described over the last decades [15, 16]. For  $[(\mathbf{L}^{1/3/4})_2\text{Ag}_4]^{2+}$  such a closed shell interaction might be rather weak if present at all, since the  $\text{Ag}\cdots\text{Ag}$  distances are well above 3.1 Å [16]. Despite the steric bulk of the peripheral *tert*-butyl or 1-adamantyl groups,  $\text{Ag}\cdots\text{Ag}$  separations are in the same range as in the sterically less demanding silver(I) complex of 3,5-bis[*N*-methylimidazolium-1-ylmethyl]-1*H*-pyrazole [9, 10]. This indicates that the *tert*-butyl or 1-adamantyl substituents do not impose any particular constraints on the  $\text{Ag}_4$  framework. On a more subtle level, it is interesting to note that two sets of  $\text{Ag}\cdots\text{Ag}$  interactions with clearly different distances can be observed in all these  $\text{Ag}_4$  complexes. In  $[(\mathbf{L}^1)_2\text{Ag}_4]^{2+}$  the difference between both sets is around 0.2 Å, while in  $[(\mathbf{L}^3)_2\text{Ag}_4]^{2+}$  and  $[(\mathbf{L}^4)_2\text{Ag}_4]^{2+}$  it is around 0.1 Å. A difference of almost 0.4 Å was reported for the silver(I) complex of 3,5-bis[3-(2,4,6-trimethylphenyl)imidazolium-1-ylmethyl]-1*H*-pyrazole, which might be indicative of a weak pairwise  $d^{10}$ - $d^{10}$  interaction for this complex. Apparently, this effect is less pronounced in the case of  $[(\mathbf{L}^1)_2\text{Ag}_4]^{2+}$ ,  $[(\mathbf{L}^3)_2\text{Ag}_4]^{2+}$  and  $[(\mathbf{L}^4)_2\text{Ag}_4]^{2+}$ . The  $\text{Ag}-\text{C}$  and  $\text{Ag}-\text{N}$  bond lengths ( $\sim 2.1$  Å) as well as the almost linear  $\text{N}-\text{Ag}-\text{C}$  angles are within the expected range. The  $\text{N}-\text{C}-\text{N}$  angle is around  $105^\circ$  and is somewhat smaller than in the protonated imidazolium salts ( $\sim 109^\circ$ ).

The most noticeable feature of the  $^1\text{H}$  NMR spectra of  $[(\mathbf{L}^1)_2\text{Ag}_4](\text{BF}_4)_2$ ,  $[(\mathbf{L}^3)_2\text{Ag}_4](\text{BF}_4)_2$  and  $[(\mathbf{L}^4)_2\text{Ag}_4](\text{PF}_6)_2$  is the absence of the  $\text{CH}^{\text{im}2}$  resonance as the imidazolium proton is replaced by a silver-carbene bond. Furthermore, the bridging  $\text{CH}_2$  groups appear as an AB system. In the  $^{13}\text{C}$  NMR

spectrum of  $[(\mathbf{L}^1)_2\text{Ag}_4](\text{BF}_4)_2$ , the carbene carbon appears as broad singlet (175 ppm) that is shifted approximately 40 ppm downfield compared to the free imidazolium salt. Broadening may indicate that the carbon-silver bond is not persistent in solution on the NMR timescale; two narrow doublets ( $^1J(^{13}\text{C}, ^{107}\text{Ag}) = 235$  Hz,  $^1J(^{13}\text{C}, ^{109}\text{Ag}) = 271$  Hz) were only observed at  $-25^\circ\text{C}$ . Similarly, the pyrazole  $^{15}\text{N}$  resonance ( $-113$  ppm) is shifted downfield by about 20 ppm and, again at low temperature, is split by the two Ag isotopes with an average coupling constant  $^1J(^{15}\text{N}, ^{107}\text{Ag})$  of 73 Hz. The  $^{109}\text{Ag}$  resonance itself is detected through  $J$  coupling with the pyrazole, imidazole and  $\text{CH}_2$  protons and appears at 634 ppm. Chemical shifts and coupling constants are in agreement with pyrazolate-NHC complexes that were previously studied in our laboratory [10].

When the reaction between  $[\text{H}_3\mathbf{L}^1](\text{PF}_6)_2$  and  $\text{Ag}_2\text{O}$  was performed in acetone instead of MeCN, a different product  $[(\text{H}_2\mathbf{L}^1)_4\text{Ag}_4](\text{PF}_6)_8$  containing four ligands and four silver ions was obtained (Scheme 2).  $^1\text{H}$  and  $^{13}\text{C}$  NMR spectra of this novel complex are distinct from those of  $[(\mathbf{L}^1)_2\text{Ag}_4]^{2+}$ : the  $^1\text{H}$  NMR signal for the  $\text{CH}_2$  linker groups shows a singlet, and the presence of a peak at 8.56 ppm illustrates that the imidazole is not coordinated to silver. NOE correlations between the pyrazole and the  $\text{CH}_2$  protons on the one hand and the proximal and isolated imidazole CH proton on the other hand show that the imidazolium groups are fully flexible in solution. Furthermore, the pyrazole  $^{15}\text{N}$  resonance remains a singlet, and the  $^{109}\text{Ag}$  resonance remains undetected down to  $-40^\circ\text{C}$ , suggesting that the nitrogen-silver bond is highly dynamic. Crystallization by slow diffusion of diethyl ether into an acetone solution of  $[(\text{H}_2\mathbf{L}^1)_4\text{Ag}_4](\text{PF}_6)_8$  at r. t. afforded colorless crystals that allowed the elucidation of its structure by X-ray diffraction (Fig. 5).

$[(\text{H}_2\mathbf{L}^1)_4\text{Ag}_4](\text{PF}_6)_8$  features a central 12-membered ring of four silver ions and four  $N,N'$ -bridging pyrazolate ligands with crystallographically imposed  $S_4$  symmetry. Cyclic  $(\text{pzAg})_n$  cores are a common structural motif in coinage metal pyrazolate complexes [11], and a similar tetrameric  $(\text{pzAg})_4$  ring has previously been observed in the silver(I) complex of 3,5-di-*tert*-butylpyrazole [17] and in **B** [10]. As concluded from the NMR spectra of  $[(\text{H}_2\mathbf{L}^1)_4\text{Ag}_4](\text{PF}_6)_8$ , the silver ions are solely bound to the pyrazolate-N atoms, while all side arm imidazolium groups are still protonated and dangling. The imidazolium- $\text{C}^2\text{H}$  shows weak hydrogen bonding or close contacts to oxygen

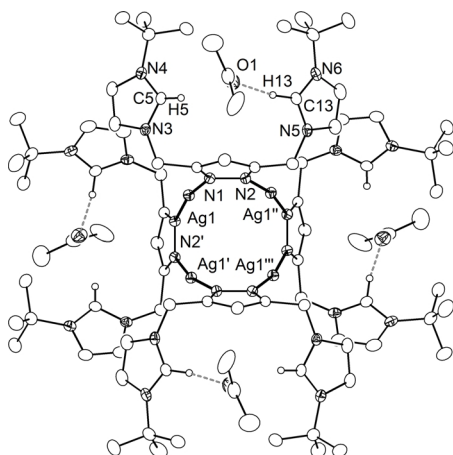


Fig. 5. ORTEP plot (30% probability displacement ellipsoids) of the cation of  $[(H_2L^1)_4Ag_4](PF_6)_8$  emphasizing the hydrogen bonding interactions. For the sake of clarity most hydrogen atoms, most solvent molecules, and  $PF_6^-$  have been omitted. Symmetry transformations used to generate equivalent atoms: (')  $y, 1.5 - x, 1.5 - z$ ; (")  $1.5 - y, x, 1.5 - z$ ; (""')  $1.5 - x, 1.5 - y, z$ . Selected parameters for hydrogen bonding or close contacts (Å; deg): C5...O1 3.778(4), C13...O1 3.231(4), C5...F11 2.933(4); C5-H5...O1 164(3), C13-H13...O1 166(4), C5-H5...F11 104(3).

atoms of neighboring acetone solvent molecules (shown in Fig. 5) or  $PF_6^-$  anions. The four silver atoms are arranged in an almost square fashion with  $Ag \cdots Ag$  distances of 3.1 Å.  $N-Ag-N$  angles ( $168^\circ$ ) deviate somewhat more from  $180^\circ$  than the  $C-Ag-N$  angles in complexes  $[(L^x)_2Ag_4]^{2+}$ .

The molecular structure of  $[(H_2L^1)_4Ag_4]^{8+}$  bears a striking resemblance to the recently reported double-crowned  $Ag_8$  complex **B**, which features the same central  $(pzAg)_4$  core but hosts four additional silver ions in the peripheral bis(NHC) compartments [10, 18]. It is thus tempting to assume that further reaction of the  $[(H_2L^1)_4Ag_4]^{8+}$  cation with  $Ag_2O$  may lead to type **B** systems *via* incorporation of additional silver(I) ions in the outer ligand sphere, potentially followed by rearrangement to yield the structural isomer  $[(L^1)_2Ag_4]^{2+}$  (type **A**). The formation of either  $[(H_2L^1)_4Ag_4]^{8+}$  or  $[(L^1)_2Ag_4]^{2+}$  appears to be solvent-dependent, since prolonged stirring of a mixture of the ligand precursor  $[H_3L^1](PF_6)_2$  and  $Ag_2O$  in acetone only gives the former complex with a 1 : 1 ligand to metal ratio, even in the presence of an excess of  $Ag_2O$ . However, when  $[(H_2L^1)_4Ag_4]^{8+}$  was treated with additional 2.2 eq. of  $Ag_2O$  for 48 h in MeCN solution, changes of the  $^1H$  NMR spectrum (in particular the disappearance of

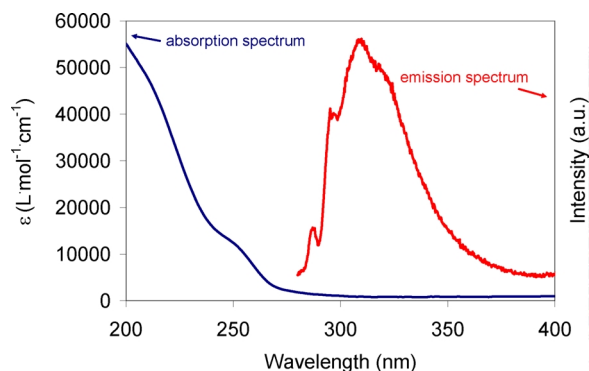


Fig. 6. Absorption spectrum and normalized emission spectrum ( $\lambda_{ex} = 265$  nm) of  $[(H_2L^1)_4Ag_4](PF_6)_8$  at r. t. in MeCN solution.

the signal at 8.56 ppm) indicated gradual transformation to  $[(L^1)_2Ag_4]^{2+}$  with a ligand to metal ratio of 1 : 2 as the final product (Scheme 2). No type **B** intermediate could be detected in this case, suggesting that the species distribution also depends on the imidazolium substituents.  $[(L^1)_2Ag_4]^{2+}$  is stable in  $[D_6]DMSO$  at r. t. for at least one month, and no particular light sensitivity was observed.

The new tetranuclear silver(I) complex  $[(H_2L^1)_4Ag_4](PF_6)_8$  displays emissive properties in solution. Its UV/Vis spectrum shows strong absorption below 240 nm with a pronounced shoulder at around 255 nm, and a broad emission band centered at around 310 nm upon excitation at  $\lambda_{ex} = 265$  nm was observed (Fig. 6). More detailed studies of the luminescence properties of the various silver(I) complexes derived from binucleating pyrazole/NHC hybrid ligands are planned for the future.

## Conclusion

A set of new compartmental pyrazolate/NHC ligands with bulky imidazolium substituents (*tert*-butyl, 1-adamantyl) and different substituents at the pyrazolate- $C^4$  backbone (H, Ph) has been prepared, and several of their pyrazole/imidazolium precursors (as  $BF_4^-$  and  $PF_6^-$  salts) have been characterized by X-ray crystallography. An interesting structural feature is that both the pyrazole-NH and the imidazolium  $C^2H$  are strongly involved in hydrogen bonding interactions. Silver(I) complexes of the ligands can be conveniently prepared by the  $Ag_2O$  route and feature either the known  $[L_2Ag_4]^{2+}$  or the new  $[(H_2L^1)_4Ag_4]^{8+}$  motif, depending on the solvent for the reaction. The latter is composed of a

central (pzAg)<sub>4</sub> ring with pendant imidazolium side arms. Upon further reaction with Ag<sub>2</sub>O in MeCN the [(H<sub>2</sub>L<sup>1</sup>)<sub>4</sub>Ag<sub>4</sub>]<sup>8+</sup> species transforms into the corresponding [(L<sup>1</sup>)<sub>2</sub>Ag<sub>4</sub>]<sup>2+</sup>. Further structural variations can likely be expected from the silver(I) chemistry of such versatile pyrazolate/NHC hybrid ligands, and preliminary data for [(H<sub>2</sub>L<sup>1</sup>)<sub>4</sub>Ag<sub>4</sub>]<sup>8+</sup> suggest that they may also exhibit interesting luminescence properties.

## Experimental Section

All reactions were carried out at r.t. under an atmosphere of dry nitrogen, using standard Schlenk line techniques. Melting points/decomposition temperatures were determined on an OptiMelt system (Stanford Research Systems, Inc.) using open capillaries; values are uncorrected. NMR spectra were recorded on a Bruker Avance 500 MHz spectrometer at r.t., and chemical shifts are reported in ppm and were referenced internally to solvent signals: CDCl<sub>3</sub> (<sup>1</sup>H: 7.24 ppm; <sup>13</sup>C: 77.0 ppm), CD<sub>3</sub>CN (<sup>1</sup>H: 1.94 ppm; <sup>13</sup>C: 1.32 ppm, 118.26 ppm) and [D<sub>6</sub>]DMSO (<sup>1</sup>H: 2.50 ppm; <sup>13</sup>C: 39.52 ppm). <sup>15</sup>N and <sup>109</sup>Ag resonances were detected and assigned with HMQC-type schemes [19] using transfer delays of 33 and 166 ms, respectively, and referenced to the unified  $\Xi$  scale [20] using  $\Xi(\text{Me}^{15}\text{NO}_2) = 10.136767$  and  $\Xi(\text{sat. }^{109}\text{AgNO}_3) = 4.653533$ . HMQC experiments with transfer delays of 33 ms were also used to assign the carbene and other quaternary carbon <sup>13</sup>C resonances. Mass spectra were recorded using an Applied Biosystems API 2000 system. Elemental analyses were performed by the analytical laboratory of the Institut für Anorganische Chemie der Universität Göttingen using an Elementar Vario EL III instrument. UV/Vis and fluorescence spectra of solutions of [(H<sub>2</sub>L<sup>1</sup>)<sub>4</sub>Ag<sub>4</sub>](PF<sub>6</sub>)<sub>8</sub> were measured with a Jasco V-550 UV/Vis spectrometer and a Jasco FP-6500 fluorescence spectrometer.

3,5-Bis(chloromethyl)-1-(tetrahydropyran-2-yl)-pyrazole [21], 3,5-bis(chloromethyl)-1-(tetrahydropyran-2-yl)-4-phenyl-1*H*-pyrazole [22] and *N*-substituted imidazoles [10] were prepared according to procedures found in the literature. All other chemicals were purchased and used as supplied.

### General procedure for the preparation of ligand precursors

A mixture of 3,5-bis(chloromethyl)-1-(tetrahydropyran-2-yl)-pyrazole (25.0 mmol, 1.0 eq.) and the respected *N*-substituted-imidazole (75.0 mmol, 3.0 eq.) in 100 mL CH<sub>3</sub>CN was heated to reflux for 48 h. After this time the solvent was removed, and the residue was dissolved in a mixture of water (100 mL) and dichloromethane (100 mL). The phases were separated, and the aqueous layer was extracted twice with dichloromethane. The excess of imidazole can be recycled from combined organic phases. Water was re-

moved from the aqueous phase under reduced pressure, and the residue was dried under vacuum. The crude product was then dissolved in ethanol (10 mL) and treated with ethanolic HCl. The solution was stirred overnight at r.t. Addition of diethyl ether (1.0 L) gave an off-white precipitate which was collected by filtration, washed with diethyl ether (200 mL) and dried *in vacuo* at 90 °C. This crude product (chloride salt) is hygroscopic and is best transformed into the hexafluorophosphate or tetrafluorophosphate salts. For this it was dissolved in as little water as possible and treated with NH<sub>3</sub> solution (25 %, 3.0 eq.). The mixture was stirred for several min, and either ammonium hexafluorophosphate (2.2 eq.) or sodium tetrafluorophosphate (2.2 eq.) was added. A precipitate instantly formed. After a reaction time of 30 min the colorless precipitate was filtered off, washed with some water and dried *in vacuo*. The product was obtained as a colorless powder.

[H<sub>3</sub>L<sup>1</sup>](BF<sub>4</sub>)<sub>2</sub>: This was prepared using the general procedure (yield of intermediate [H<sub>4</sub>L<sup>1</sup>]Cl<sub>3</sub>: 79 %; yield of [H<sub>3</sub>L<sup>1</sup>](BF<sub>4</sub>)<sub>2</sub>: 20 % based on [H<sub>4</sub>L<sup>1</sup>]Cl<sub>3</sub>; yield of the corresponding [H<sub>3</sub>L<sup>1</sup>](PF<sub>6</sub>)<sub>2</sub> was 90 % based on [H<sub>4</sub>L<sup>1</sup>]Cl<sub>3</sub>). Colorless crystals were obtained by slow diffusion of diethyl ether into a CH<sub>3</sub>OH solution of [H<sub>3</sub>L<sup>1</sup>](BF<sub>4</sub>)<sub>2</sub> at r.t. M.p. 203 °C. – <sup>1</sup>H NMR (500.14 MHz, [D<sub>6</sub>]DMSO):  $\delta = 1.57$  (s, 9 H, *t*Bu), 1.58 (s, 9 H, *t*Bu), 5.36 (s, 2 H, CH<sub>2</sub>), 5.46 (s, 2 H, CH<sub>2</sub>), 6.47 (d, *J* = 1.3 Hz, 1 H, CH<sup>pz</sup>), 7.74 (t, *J* = 1.6 Hz, 1 H, CH<sup>im</sup>), 7.76 (t, *J* = 1.6 Hz, 1 H, CH<sup>im</sup>), 7.99 (t, *J* = 1.6 Hz, 1 H, CH<sup>im</sup>), 8.03 (t, *J* = 1.6 Hz, 1 H, CH<sup>im</sup>), 9.30 (t, *J* = 1.6 Hz, 1 H, CH<sup>im2</sup>), 9.36 (t, *J* = 1.6 Hz, 1 H, CH<sup>im2</sup>), 13.18 (br s, 1 H, NH). – <sup>13</sup>C NMR (125.77 MHz, [D<sub>6</sub>]DMSO):  $\delta = 28.9, 28.9$  (2 × *t*Bu), 43.1, 46.1 (2 × CH<sub>2</sub>), 59.7, 59.8 (2 × C<sup>*t*Bu</sup>), 104.9 (CH<sup>pz4</sup>), 120.4, 120.8, 122.5, 122.8 (all CH<sup>im</sup>), 134.6, 134.8 (2 × CH<sup>im2</sup>), 137.7 (C<sup>pz5</sup>), 146.1 (C<sup>pz3</sup>). – MS ((+)-ESI): *m/z* (%) = 429 (20) [M–BF<sub>4</sub>]<sup>+</sup>, 341 (19) [M–2BF<sub>4</sub>–H]<sup>+</sup>, 229 (69) [M–2BF<sub>4</sub>–2*t*Bu–H]<sup>+</sup>, 161 (100) [M–2BF<sub>4</sub>–2*t*Bu–im]<sup>+</sup>, 69 (40) [im+H]<sup>+</sup>. – MS ((–)-ESI): *m/z* (%) = 87 (100) [BF<sub>4</sub>]<sup>–</sup>. – C<sub>19</sub>H<sub>30</sub>B<sub>2</sub>F<sub>8</sub>N<sub>6</sub> (516.09): calcd. C 44.22, H 5.86, N 16.28; found C 43.98, H 5.88, N 16.48.

[H<sub>3</sub>L<sup>2</sup>](PF<sub>6</sub>)<sub>2</sub>: This was prepared using the general procedure (yield of intermediate [H<sub>4</sub>L<sup>2</sup>]Cl<sub>3</sub>: 82 %; yield of [H<sub>3</sub>L<sup>2</sup>](PF<sub>6</sub>)<sub>2</sub>: 93 % based on [H<sub>4</sub>L<sup>2</sup>]Cl<sub>3</sub>). – <sup>1</sup>H NMR (500.14 MHz, [D<sub>6</sub>]DMSO):  $\delta = 1.46$  (s, 18 H, *t*Bu), 5.47 (s, 4 H, CH<sub>2</sub>), 7.18 (m, 2 H, CH<sup>*o*-ph</sup>), 7.36 (m, 3 H, CH<sup>*m,p*-ph</sup>), 7.53 (t, *J* = 1.8 Hz, 2 H, CH<sup>im</sup>), 7.88 (t, *J* = 1.8 Hz, 2 H, CH<sup>im</sup>), 9.10 (br s, 2 H, CH<sup>im2</sup>), 13.44 (br s, 1 H, NH). – <sup>13</sup>C NMR (125.77 MHz, [D<sub>6</sub>]DMSO):  $\delta = 28.8$  (*t*Bu), 43.0 (br, CH<sub>2</sub>), 45.2 (br, CH<sub>2</sub>), 59.6 (C<sup>*t*Bu</sup>), 119.0 (C<sup>pz4</sup>), 120.4 (CH<sup>im</sup>), 122.7 (CH<sup>im</sup>), 127.6 (CH<sup>*p*-ph</sup>), 128.8 (CH<sup>*m*-ph</sup>), 129.1 (CH<sup>*o*-ph</sup>), 130.2 (CH<sup>*i*-ph</sup>), 134.8 (CH<sup>im2</sup>), 143.6 (C<sup>pz3,5</sup>). – MS ((+)-ESI): *m/z* (%) = 563 (28) [M–PF<sub>6</sub>]<sup>+</sup>, 417 (5) [M–2PF<sub>6</sub>–H]<sup>+</sup>, 361 (47) [M–2PF<sub>6</sub>–H–*t*Bu]<sup>+</sup>, 181 (100). – MS ((–)-ESI): *m/z* (%) = 145 (100) [PF<sub>6</sub>]<sup>–</sup>.

$[\text{H}_3\text{L}^3](\text{BF}_4)_2$ : This was prepared using the general procedure (yield of intermediate  $[\text{H}_4\text{L}^3]\text{Cl}_3$ : 98%; yield of  $[\text{H}_3\text{L}^3](\text{BF}_4)_2$ : 68% based on  $[\text{H}_4\text{L}^3]\text{Cl}_3$ ; the yield of the corresponding  $[\text{H}_3\text{L}^3](\text{PF}_6)_2$  was 74% based on  $[\text{H}_4\text{L}^3]\text{Cl}_3$ ). Colorless crystals were obtained by slow diffusion of diethyl ether into a methanol solution of  $[\text{H}_3\text{L}^3](\text{BF}_4)_2$  at r. t. M. p. 233 °C. –  $^1\text{H}$  NMR (500.13 MHz,  $[\text{D}_6]\text{DMSO}$ ):  $\delta$  = 1.71 (m, 12 H,  $\text{CH}_2^{\text{ad}}$ ), 2.10 (m, 12 H,  $\text{CH}_2^{\text{ad}}$ ), 2.21 (m, 6 H,  $\text{CH}^{\text{ad}}$ ), 5.36 (s, 2 H,  $\text{CH}_2$ ), 5.46 (s, 2 H,  $\text{CH}_2$ ), 6.46 (s, 1 H,  $\text{CH}^{\text{pz}}$ ), 7.77 (s, 2 H,  $\text{CH}^{\text{im}}$ ), 8.03 (s, 1 H,  $\text{CH}^{\text{im}}$ ), 8.06 (s, 1 H,  $\text{CH}^{\text{im}}$ ), 9.35 (s, 1 H,  $\text{CH}^{\text{im}2}$ ), 9.38 (s, 1 H,  $\text{CH}^{\text{im}2}$ ), 13.23 (br s, 1 H,  $\text{NH}$ ). –  $^{13}\text{C}$  NMR (125.77 MHz,  $[\text{D}_6]\text{DMSO}$ ):  $\delta$  = 28.8 ( $\text{CH}^{\text{ad}}$ ), 34.8 ( $\text{CH}-\text{CH}_2-\text{CH}^{\text{ad}}$ ), 41.5, 41.5 ( $2 \times \text{C}-\text{CH}_2^{\text{ad}}$ ), 43.1, 46.2 ( $2 \times \text{CH}_2$ ), 59.3, 59.4 ( $2 \times \text{C}^{\text{ad}}$ ), 104.9 ( $\text{CH}^{\text{pz}4}$ ), 119.5, 119.8, 122.5, 122.8 (all  $\text{CH}^{\text{im}}$ ), 134.1, 134.4 ( $2 \times \text{CH}^{\text{im}2}$ ), 137.6 ( $\text{CH}^{\text{pz}5}$ ), 146.1 ( $\text{CH}^{\text{pz}3}$ ). – MS ((+)-ESI):  $m/z$  (%) = 585 (18)  $[\text{M}-\text{BF}_4]^+$ , 363 (100)  $[\text{M}-2\text{BF}_4-\text{ad}]^+$ , 135 (85)  $[\text{ad}]^+$ . – MS ((–)-ESI):  $m/z$  (%) = 87 (100)  $[\text{BF}_4]^-$ . –  $\text{C}_{31}\text{H}_{42}\text{B}_2\text{F}_8\text{N}_6$  (672.31): calcd. C 55.38, H 6.29, N 12.50; found C 54.91, H 6.18, N 12.52.

$[\text{H}_3\text{L}^4](\text{PF}_6)_2$ : This was prepared using the general procedure (yield of intermediate  $[\text{H}_4\text{L}^4]\text{Cl}_3$ : 22%; yield of  $[\text{H}_3\text{L}^4](\text{PF}_6)_2$ : 84% based on  $[\text{H}_4\text{L}^4]\text{Cl}_3$ ). Colorless crystals were obtained by slow diffusion of diethyl ether into a  $\text{CH}_3\text{CN}/\text{CH}_3\text{OH}$  solution of  $[\text{H}_3\text{L}^4](\text{PF}_6)_2$  at r. t. M. p. 209 °C. –  $^1\text{H}$  NMR (500.14 MHz,  $[\text{D}_6]\text{DMSO}$ ):  $\delta$  = 1.67 (m, 12 H,  $\text{CH}_2^{\text{ad}}$ ), 1.95 (d,  $J$  = 2.5 Hz, 12 H,  $\text{CH}_2^{\text{ad}}$ ), 2.18 (m, 6 H,  $\text{CH}^{\text{ad}}$ ), 5.47 (s, 4 H,  $\text{CH}_2$ ), 7.17 (m, 2 H,  $\text{CH}^{\text{o-ph}}$ ), 7.37 (m, 3 H,  $\text{CH}^{\text{m-p-ph}}$ ), 7.53 (t,  $J$  = 1.8 Hz, 2 H,  $\text{CH}^{\text{im}}$ ), 7.92 (t,  $J$  = 1.8 Hz, 2 H,  $\text{CH}^{\text{im}}$ ), 9.10 (t,  $J$  = 1.6 Hz, 2 H,  $\text{CH}^{\text{im}2}$ ), 13.55 (br s, 1 H,  $\text{NH}$ ). –  $^{13}\text{C}$  NMR (125.77 MHz,  $[\text{D}_6]\text{DMSO}$ ):  $\delta$  = 28.8 ( $\text{CH}^{\text{ad}}$ ), 28.9 ( $\text{CH}-\text{CH}_2-\text{CH}^{\text{ad}}$ ), 41.4 ( $\text{C}-\text{CH}_2^{\text{ad}}$ ), 44.2 (br,  $\text{CH}_2$ ), 59.2 ( $\text{C}^{\text{ad}}$ ), 119.0 ( $\text{CH}^{\text{pz}4}$ ), 119.5, 122.7 ( $2 \times \text{CH}^{\text{im}}$ ), 127.6 ( $\text{CH}^{\text{p-ph}}$ ), 128.8 ( $\text{CH}^{\text{m-ph}}$ ), 129.0 ( $\text{CH}^{\text{o-ph}}$ ), 130.3 ( $\text{CH}^{\text{i-ph}}$ ), 134.3 ( $\text{CH}^{\text{im}2}$ ). – MS ((+)-ESI):  $m/z$  (%) = 719 (18)  $[\text{M}-\text{PF}_6]^+$ , 440 (70)  $[\text{M}-2\text{PF}_6-\text{ad}+\text{H}]^+$ , 135 (100)  $[\text{ad}]^+$ . –  $\text{C}_{74}\text{H}_{91}\text{F}_{18}\text{N}_{12}\text{P}_3 \times 0.5 \text{CH}_3\text{CN} \times 0.5 \text{H}_2\text{O}$  (1613.02): calcd. C 55.84, H 5.84, N 10.85; found C 55.80, H 6.03, N 10.87.

*General procedure for the preparation of silver complexes  $[(\text{L}^x)_2\text{Ag}_4](\text{PF}_6)_2$  and  $[(\text{L}^x)_2\text{Ag}_4](\text{BF}_4)_2$*

A solution of the ligand precursor  $[\text{H}_3\text{L}^x](\text{PF}_6)_2$  or  $[\text{H}_3\text{L}^x](\text{BF}_4)_2$  (1.0 eq.) in MeCN was treated with  $\text{Ag}_2\text{O}$  (2.2 eq.), and the mixture was stirred for 48 h at r. t. under exclusion of light. The reaction mixture was filtrated through activated carbon and Celite 545 to remove unreacted  $\text{Ag}_2\text{O}$ , yielding a clear solution. After removal of the solvent under reduced pressure a solid was obtained. Crystals suitable for X-ray diffraction analysis were obtained by slow diffusion of diethyl ether into a solution of the crude product at r. t.

$[(\text{L}^1)_2\text{Ag}_4](\text{BF}_4)_2$ : Starting from  $[\text{H}_3\text{L}^1](\text{BF}_4)_2$  (1.00 g, 2.23 mmol) and following the general procedure yielded 0.44 g (0.34 mmol, 15%) of the product. Crystallization by slow diffusion of diethyl ether into a  $\text{CH}_3\text{CN}/\text{CH}_3\text{OH}$  (5 : 1) solution of  $[(\text{L}^1)_2\text{Ag}_4](\text{BF}_4)_2$  at r. t. afforded colorless crystals. M. p. 262 °C (dec.). –  $^1\text{H}$  NMR (500.13 MHz,  $\text{CD}_3\text{CN}$ ):  $\delta$  = 1.62 (s, 18 H,  $t\text{Bu}$ ), 5.19 (d,  $J$  = 15.1 Hz, 2 H,  $\text{CH}_2$ ), 5.32 (d,  $J$  = 15.1 Hz, 2 H,  $\text{CH}_2$ ), 6.18 (s, 1 H,  $\text{CH}^{\text{pz}}$ ), 7.32 (d,  $J$  = 1.9 Hz, 2H,  $\text{CH}^{\text{im}}$ ), 7.33 (d,  $J$  = 1.9 Hz, 2 H,  $\text{CH}^{\text{im}}$ ). –  $^1\text{H}$  NMR (500.13 MHz,  $[\text{D}_6]\text{DMSO}$ ):  $\delta$  = 1.59 (s, 18 H,  $t\text{Bu}$ ), 5.31 (d,  $J$  = 14.8 Hz, 2 H,  $\text{CH}_2$ ), 5.45 (d,  $J$  = 14.8 Hz, 2 H,  $\text{CH}_2$ ), 6.27 (s, 1 H,  $\text{CH}^{\text{pz}}$ ), 7.61 (d,  $J$  = 1.8 Hz, 2 H,  $\text{CH}^{\text{im}}$ ), 7.66 (d,  $J$  = 1.8 Hz, 2 H,  $\text{CH}^{\text{im}}$ ). –  $^{13}\text{C}$  NMR (125.77 MHz,  $\text{CD}_3\text{CN}$ ):  $\delta$  = 32.0 ( $t\text{Bu}$ ), 50.5 ( $\text{CH}_2$ ), 58.8 ( $\text{C}^{\text{tBu}}$ ), 103.7 ( $\text{CH}^{\text{pz}4}$ ), 119.4, 123.3 ( $2 \times \text{CH}^{\text{im}}$ ), 154.1 ( $\text{C}^{\text{pz}3,5}$ ), 175.5 (br,  $\text{Ag}-\text{C}^{\text{im}}$ ). –  $^{13}\text{C}$  NMR (125.77 MHz,  $[\text{D}_6]\text{DMSO}$ ):  $\delta$  = 31.2 ( $t\text{Bu}$ ), 48.8 ( $\text{CH}_2$ ), 57.5 ( $\text{C}^{\text{tBu}}$ ), 103.1 ( $\text{CH}^{\text{pz}4}$ ), 118.9, 122.8 ( $2 \times \text{CH}^{\text{im}}$ ), 152.8 ( $\text{C}^{\text{pz}3,5}$ ), 173.5 (br d,  $J$  = 250 Hz,  $\text{Ag}-\text{C}^{\text{im}}$ ). –  $^{15}\text{N}$  NMR (40.56 MHz,  $\text{CD}_3\text{CN}$ ):  $\delta$  = –184.2, –161.7 ( $2 \times \text{N}^{\text{im}}$ ), –113.4 (br,  $\text{N}^{\text{pz}}$ ). – MS ((+)-ESI):  $m/z$  = 1197 (3.3)  $[\text{M}-\text{BF}_4]^+$ , 1109 (0.5)  $[\text{M}-2\text{BF}_4-\text{H}]^+$ , 555 (100),  $[\text{Ag}_2\text{L}^1]^+$ . – MS ((–)-ESI):  $m/z$  (%) = 87 (100)  $[\text{BF}_4]^-$ . – UV/Vis:  $\lambda$  = 249, 226, 203 nm. –  $\text{C}_{38}\text{H}_{54}\text{Ag}_4\text{B}_2\text{F}_8\text{N}_{12}$  (1284.00): calcd. C 35.54, H 4.24, N 13.09; found C 35.28, H 4.53, N 13.08.

$[(\text{L}^3)_2\text{Ag}_4](\text{BF}_4)_2$ : Starting from  $[\text{H}_3\text{L}^3](\text{BF}_4)_2$  (0.75 g, 1.12 mmol) and following the general procedure yielded 0.99 g (0.63 mmol, 56%) of the product. Crystallization by slow diffusion of diethyl ether into a  $\text{CH}_3\text{CN}$  solution of  $[(\text{L}^3)_2\text{Ag}_4](\text{BF}_4)_2$  at r. t. afforded colorless crystals. –  $^1\text{H}$  NMR (500.14 MHz,  $\text{CD}_3\text{CN}$ ):  $\delta$  = 1.66 (d,  $J$  = 12.6 Hz, 6 H,  $\text{CH}_2^{\text{ad}}$ ), 1.74 (d,  $J$  = 12.6 Hz, 6 H,  $\text{CH}_2^{\text{ad}}$ ), 2.14 (m, 6 H,  $\text{CH}^{\text{ad}}$ ), 2.23 (m, 12 H,  $\text{CH}_2^{\text{ad}}$ ), 5.18 (d,  $J$  = 15.1 Hz, 2 H,  $\text{CH}_2$ ), 5.32 (d,  $J$  = 15.1 Hz, 2 H,  $\text{CH}_2$ ), 6.18 (s, 1 H,  $\text{CH}^{\text{pz}}$ ), 7.32 (d,  $J$  = 1.8 Hz, 2 H,  $\text{CH}^{\text{im}}$ ), 7.34 (d,  $J$  = 1.8 Hz, 2 H,  $\text{CH}^{\text{im}}$ ). –  $^{13}\text{C}$  NMR (125.77 MHz,  $\text{CD}_3\text{CN}$ ):  $\delta$  = 30.9 ( $\text{CH}^{\text{ad}}$ ), 36.3 ( $\text{CH}-\text{CH}_2-\text{CH}^{\text{ad}}$ ), 45.5 ( $\text{C}-\text{CH}_2^{\text{ad}}$ ), 50.7 ( $\text{CH}_2$ ), 59.1 ( $\text{C}^{\text{ad}}$ ), 103.8 ( $\text{CH}^{\text{pz}4}$ ), 118.5, 123.3 ( $2 \times \text{CH}^{\text{im}}$ ), 154.2 ( $\text{C}^{\text{pz}3,5}$ ). – MS ((+)-ESI):  $m/z$  = 1509 (0.9)  $[\text{M}-\text{BF}_4]^+$ , 711 (100)  $[\text{M}-2\text{BF}_4]^2+$ , 363 (46)  $[\text{L}^3-\text{ad}]^+$ , 135 (38)  $[\text{ad}]^+$ . – MS ((–)-ESI):  $m/z$  (%) = 87 (100)  $[\text{BF}_4]^-$ .

$[(\text{L}^4)_2\text{Ag}_4](\text{PF}_6)_2$ : Starting from  $[\text{H}_3\text{L}^4](\text{PF}_6)_2$  (0.58 g, 0.67 mmol) and following the general procedure yielded 0.71 g (0.38 mmol, 57%) of the product. Crystallization by slow diffusion of diethyl ether into a  $\text{CH}_3\text{CN}$  solution of  $[(\text{L}^4)_2\text{Ag}_4](\text{PF}_6)_2$  at r. t. afforded colorless crystals. –  $^1\text{H}$  NMR (500.14 MHz,  $\text{CD}_3\text{CN}$ ):  $\delta$  = 1.71 (d,  $J$  = 12.5 Hz, 6 H,  $\text{CH}_2^{\text{ad}}$ ), 1.78 (d,  $J$  = 12.5 Hz, 6 H,  $\text{CH}_2^{\text{ad}}$ ), 2.20 (m, 6 H,  $\text{CH}^{\text{ad}}$ ), 2.26 (m, 12 H,  $\text{CH}_2^{\text{ad}}$ ), 5.18 (d,  $J$  = 15.4 Hz, 2 H,  $\text{CH}_2$ ), 5.25 (d,  $J$  = 15.4 Hz, 2 H,  $\text{CH}_2$ ), 6.37 (m, 2 H,  $\text{CH}^{\text{o-ph}}$ ), 6.66 (d,  $J$  = 1.9 Hz, 2 H,  $\text{CH}^{\text{im}}$ ),

Table 2. Crystal structure data for [H<sub>3</sub>L<sup>1</sup>](BF<sub>4</sub>)<sub>2</sub>, [H<sub>3</sub>L<sup>3</sup>](BF<sub>4</sub>)<sub>2</sub>, and [H<sub>3</sub>L<sup>4</sup>][H<sub>2</sub>L<sup>4</sup>](PF<sub>6</sub>)<sub>3</sub>.

	[H <sub>3</sub> L <sup>1</sup> ](BF <sub>4</sub> ) <sub>2</sub>	[H <sub>3</sub> L <sup>3</sup> ](BF <sub>4</sub> ) <sub>2</sub>	[H <sub>3</sub> L <sup>4</sup> ][H <sub>2</sub> L <sup>4</sup> ](PF <sub>6</sub> ) <sub>3</sub>
Formula	C <sub>19</sub> H <sub>30</sub> B <sub>2</sub> F <sub>8</sub> N <sub>6</sub>	C <sub>31</sub> H <sub>42</sub> B <sub>2</sub> F <sub>8</sub> N <sub>6</sub>	C <sub>75</sub> H <sub>93.5</sub> F <sub>18</sub> N <sub>12.5</sub> O <sub>0.5</sub> P <sub>3</sub>
<i>M<sub>r</sub></i>	516.11	672.33	1613.03
Crystal size, mm <sup>3</sup>	0.50 × 0.50 × 0.13	0.50 × 0.09 × 0.09	0.50 × 0.48 × 0.38
Crystal system	monoclinic	monoclinic	triclinic
Space group	<i>P</i> 2 <sub>1</sub> / <i>n</i>	<i>P</i> 2 <sub>1</sub> / <i>c</i>	<i>P</i> 1
<i>a</i> , Å	8.8998(8)	6.3306(3)	8.1576(2)
<i>b</i> , Å	15.5914(15)	20.0619(9)	15.8291(4)
<i>c</i> , Å	9.7535(10)	12.6972(6)	16.3184(4)
<i>α</i> , deg	90	90	62.919(2)
<i>β</i> , deg	116.356(7)	95.184(4)	83.780(2)
<i>γ</i> , deg	90	90	87.391(2)
<i>V</i> , Å <sup>3</sup>	1212.7(2)	1606.00(13)	1865.07(8)
<i>Z</i>	2	2	1
<i>D</i> <sub>calcd</sub> , g cm <sup>-3</sup>	1.41	1.39	1.44
<i>μ</i> (MoK <sub>α</sub> ), cm <sup>-1</sup>	0.1	0.1	0.2
<i>F</i> (000), e	536	704	842
<i>T</i> <sub>max/min</sub>	0.921 / 0.576	0.939 / 0.814	0.973 / 0.768
<i>hkl</i> range	-11 ≤ <i>h</i> ≤ +11 -19 ≤ <i>k</i> ≤ +19 -12 ≤ <i>l</i> ≤ +12	-7 ≤ <i>h</i> ≤ +8 -25 ≤ <i>k</i> ≤ +25 -16 ≤ <i>l</i> ≤ +16	-10 ≤ <i>h</i> ≤ +10 -19 ≤ <i>k</i> ≤ +20 -20 ≤ <i>l</i> ≤ +20
<i>θ</i> range	2.58–26.79	1.90–26.96	1.41–26.73
Refl. measured	13388	18523	53741
Refl. unique	2577	3477	15140
<i>R</i> <sub>int</sub>	0.0601	0.0510	0.0374
Param. refined	204	251	1016
<i>R</i> ( <i>F</i> )/ <i>wR</i> ( <i>F</i> <sup>2</sup> ) (all refl.)	0.0652 / 0.1789	0.1255 / 0.2580	0.0491 / 0.1419
<i>x</i> (Flack)	–	–	0.19(7)
GoF ( <i>F</i> <sup>2</sup> )	1.042	1.180	1.066
<i>Δρ</i> <sub>fin</sub> (max / min), e Å <sup>-3</sup>	0.58 / -0.38	0.56 / -0.45	1.07 / -0.46

7.05 (d, *J* = 1.9 Hz, 2 H, CH<sup>im</sup>), 7.11 (m, 2 H, CH<sup>m-ph</sup>), 7.17 (m, 1 H, CH<sup>p-ph</sup>). – <sup>13</sup>C NMR (125.77 MHz, CD<sub>3</sub>CN): *δ* = 30.9 (CH<sup>ad</sup>), 36.3 (CH-CH<sub>2</sub>-CH<sup>ad</sup>), 45.5 (C-CH<sub>2</sub><sup>ad</sup>), 50.2 (CH<sub>2</sub>), 60.0 (C<sup>ad</sup>), 118.1 (CH<sup>im</sup>), 121.3 (C<sup>pz4</sup>), 123.3 (CH<sup>im</sup>), 127.9 (CH<sup>p-ph</sup>), 129.2 (CH<sup>m-ph</sup>), 130.1 (CH<sup>o-ph</sup>), 132.4 (CH<sup>i-ph</sup>), 151.4 (C<sup>pz3,5</sup>). – MS ((+)-ESI): *m/z* = 1719 (1.4) [M-PF<sub>6</sub>]<sup>+</sup>, 787 (100) [M-2PF<sub>6</sub>]<sup>2+</sup>, 439 (16) [L<sup>4</sup>-ad]<sup>+</sup>, 135 (33) [ad]<sup>+</sup>. – MS ((-)-ESI): *m/z* (%) = 145 (100) [PF<sub>6</sub>]<sup>-</sup>. – C<sub>74</sub>H<sub>86</sub>Ag<sub>4</sub>F<sub>12</sub>N<sub>12</sub>P<sub>2</sub> (1864.96): calcd. C 47.66, H 4.65, N 9.01; found C 47.52, H 4.71, N 8.98.

[(H<sub>2</sub>L<sup>1</sup>)<sub>4</sub>Ag<sub>4</sub>](PF<sub>6</sub>)<sub>2</sub>: A solution of the ligand precursor [H<sub>3</sub>L<sup>1</sup>](PF<sub>6</sub>)<sub>2</sub> (3.00 g, 4.74 mmol) in acetone was treated with Ag<sub>2</sub>O (2.2 eq.), and the mixture was stirred for 48 h at r.t. under exclusion of light. The reaction mixture was filtrated through activated carbon and Celite 545 to remove unreacted Ag<sub>2</sub>O, yielding a clear solution. After removal of the solvent under reduced pressure a solid was obtained. Colorless crystals suitable for X-ray diffraction analysis were obtained by slow diffusion of diethyl ether into an acetone solution of the crude product at r.t. (1.16 g, 0.39 mmol, 9%). *M. p.* 219 °C (dec.). – <sup>1</sup>H NMR (500.14 MHz, CD<sub>3</sub>CN): *δ* = 1.59 (s, 18H, *t*Bu), 5.39 (s, 4 H, CH<sub>2</sub>), 6.44 (s, 1 H, CH<sup>pz</sup>), 7.35 (t, *J* = 1.6 Hz, 2 H, CH<sup>im</sup>), 7.56 (t, *J* = 1.8 Hz, 2 H, CH<sup>im</sup>), 8.55 (t, *J* = 1.6 Hz,

2 H, CH<sup>im2</sup>). – <sup>13</sup>C NMR (125.77 MHz, CD<sub>3</sub>CN): *δ* = 29.6 (*t*Bu), 48.2 (br, CH<sub>2</sub>), 61.4 (C<sup>*t*Bu</sup>), 104.8 (CH<sup>pz</sup>), 121.4, 123.3 (2 × CH<sup>im</sup>), 134.7 (CH<sup>im2</sup>), 148.4 (br, C<sup>pz3,5</sup>). – <sup>15</sup>N NMR (40.56 MHz, CD<sub>3</sub>CN): *δ* = -200.3, -174.8 (2 × N<sup>im</sup>), -110.3 (N<sup>pz</sup>). – MS ((+)-ESI): *m/z* = 555 (5) [Ag<sub>2</sub>L<sup>1</sup>]<sup>+</sup>, 341 (27) [L<sup>1</sup>-H]<sup>+</sup>, 285 (100) [L<sup>1</sup>-H-*t*Bu]<sup>+</sup>, 229 (98) [L<sup>1</sup>-H-2*t*Bu]<sup>+</sup>. – MS ((-)-ESI): *m/z* (%) = 145 (100) [PF<sub>6</sub>]<sup>-</sup>. – C<sub>76</sub>H<sub>116</sub>Ag<sub>4</sub>F<sub>48</sub>N<sub>24</sub>P<sub>8</sub> × 3 acetone (3145.33): calcd. C 32.60, H 4.31, N 10.73; found C 32.14, H 4.37, N 10.64.

#### Crystal structure determinations

Crystal data and details of the data collections for [H<sub>3</sub>L<sup>1</sup>](BF<sub>4</sub>)<sub>2</sub>, [H<sub>3</sub>L<sup>3</sup>](BF<sub>4</sub>)<sub>2</sub>, and [H<sub>3</sub>L<sup>4</sup>][H<sub>2</sub>L<sup>4</sup>](PF<sub>6</sub>)<sub>3</sub> as well as for [(L<sup>1</sup>)<sub>2</sub>Ag<sub>4</sub>](BF<sub>4</sub>)<sub>2</sub>, [(L<sup>3</sup>)<sub>2</sub>Ag<sub>4</sub>](BF<sub>4</sub>)<sub>2</sub>, [(L<sup>4</sup>)<sub>2</sub>Ag<sub>4</sub>](PF<sub>6</sub>)<sub>2</sub> and [(H<sub>2</sub>L<sup>1</sup>)<sub>4</sub>Ag<sub>4</sub>](PF<sub>6</sub>)<sub>8</sub> are given in Tables 2 and 3. X-Ray data were collected on a Stoe IPDS II diffractometer (graphite-monochromatized MoK<sub>α</sub> radiation, *λ* = 0.71073 Å) by use of *ω* scans at -140 °C. The structures were solved by Direct Methods and refined on *F*<sup>2</sup> using all reflections with SHELXL-97 [23]. Most non-hydrogen atoms were refined anisotropically. Most hydrogen atoms were placed in calculated positions and assigned to an isotropic displacement parameter

Table 3. Crystal structure data for  $[(L^1)_2Ag_4](BF_4)_2$ ,  $[(L^3)_2Ag_4](BF_4)_2$ ,  $[(L^4)_2Ag_4](PF_6)_2$ , and  $[(H_2L^1)_4Ag_4](PF_6)_8$ .

	$[(L^1)_2Ag_4](BF_4)_2$	$[(L^3)_2Ag_4](BF_4)_2$	$[(L^4)_2Ag_4](PF_6)_2$	$[(H_2L^1)_4Ag_4](PF_6)_8$
Formula	$C_{38}H_{54}Ag_4B_2F_8N_{12} \cdot 4MeCN \cdot MeOH$	$C_{62}H_{78}Ag_4B_2F_8N_{12} \cdot 2MeCN$	$C_{74}H_{86}Ag_4F_{12}N_{12}P_2 \cdot 6MeCN$	$C_{76}H_{116}Ag_4F_{48}N_{24}P_8 \cdot 6.5acetone \cdot 0.5H_2O$
$M_r$	1398.18	1678.57	2111.29	3343.68
Crystal size, mm <sup>3</sup>	0.30 × 0.25 × 0.21	0.38 × 0.11 × 0.10	0.50 × 0.39 × 0.18	0.50 × 0.31 × 0.26
Crystal system	triclinic	orthorhombic	monoclinic	tetragonal
Space group	$P\bar{1}$	$Pbcn$	$P2_1/c$	$P4_2/n$
$a$ , Å	9.8079(7)	22.7728(7)	15.8420(4)	23.9767(3)
$b$ , Å	11.2589(10)	12.7975(3)	11.7582(2)	23.9767(3)
$c$ , Å	14.0225(11)	23.1248(5)	23.4821(6)	12.9280(2)
$\alpha$ , deg	113.047(6)	90	90	90
$\beta$ , deg	94.447(6)	90	98.188(2)	90
$\gamma$ , deg	95.379(6)	90	90	90
$V$ , Å <sup>3</sup>	1407.51(19)	6739.4(3)	4329.50(17)	7432.08(17)
$Z$	1	4	2	2
$D_{calcd}$ , g cm <sup>-3</sup>	1.65	1.65	1.62	1.49
$\mu(MoK\alpha)$ , cm <sup>-1</sup>	1.4	1.2	1.0	0.7
$F(000)$ , e	698	3392	2144	3386
$T_{max/min}$	0.846 / 0.724	0.912 / 0.596	0.749 / 0.486	0.822 / 0.656
$hkl$ range	$-12 \leq h \leq +12$ $-14 \leq k \leq +14$ $-17 \leq l \leq +17$	$-29 \leq h \leq +29$ $-16 \leq k \leq +16$ $-24 \leq l \leq +29$	$-20 \leq h \leq +20$ $-14 \leq k \leq +13$ $-29 \leq l \leq +29$	$-30 \leq h \leq +30$ $-30 \leq k \leq +30$ $-15 \leq l \leq +16$
$\theta$ range	1.59–26.86	1.79–27.00	1.30–26.73	1.70–26.74
Refl. measured	16602	59621	38689	82407
Refl. unique	5983	7087	9155	7902
$R_{int}$	0.0490	0.0941	0.0241	0.0522
Param. refined	379	481	553	472
$R(F)/wR(F^2)$ (all refl.)	0.0566 / 0.1463	0.0450 / 0.0920	0.0243 / 0.0654	0.0350 / 0.1063
GoF ( $F^2$ )	1.001	1.038	1.077	1.051
$\Delta\rho_{fin}$ (max / min), e Å <sup>-3</sup>	3.38 (near Ag1) / -0.67	1.14 / -0.62	0.78 / -0.62	0.57 / -0.58

of 0.08 Å<sup>2</sup>. The positional and isotropic displacement parameters of the imidazolium-C5-bound hydrogen atom in  $[H_3L^1](BF_4)_2$  and the imidazolium-C5/13-bound hydrogen atoms in  $[(H_2L^1)_4Ag_4](PF_6)_8$  were refined without any restraints or constraints. A fixed isotropic displacement parameter of 0.08 Å<sup>2</sup> was assigned to the nitrogen-bound hydrogen atom H2 and the imidazolium-C11/25/51/65-bound hydrogen atoms in  $[H_3L^4][H_2L^4](PF_6)_3$ . The positional parameters were refined without any restraints. In  $[H_3L^1](BF_4)_2$  and  $[H_3L^3](BF_4)_2$  the central pyrazole moiety is disordered about a center of inversion and was refined at half occupancy. SADI restraints ( $d_{C-C}/d_{N-C}$ ) were used to model the disorder. Additionally the  $BF_4^-$  anions in these compounds were found to be disordered and were refined using SADI ( $d_{B-F}$  and  $d_{F...F}$ ) restraints and EADP constraints. A similar disorder for  $BF_4^-$  was determined in  $[(L^1)_2Ag_4](BF_4)_2$  and was refined in an equal manner. In the same compound one *tert*-butyl group was found to be disordered, as was methanol. The latter solvent molecule is disordered about two positions and additionally situated on a center of inversion. The occupancy was set to 0.25, and DFIX restraints ( $d_{C-O} = 1.42$  Å) were applied. In  $[(H_2L^1)_4Ag_4](PF_6)_8$  both acetone and H<sub>2</sub>O were found to be disordered about the 4-

fold rotation axis. The occupancy of both molecules was set to 0.125 and DFIX ( $d_{C-C} = 1.4$  Å,  $d_{C-O} = 1.2$  Å,  $d_{C...C} = 2.5$  Å), and FLAT restraints were used to model the disorder. Hydrogen atoms bound to the oxygen atom of the water molecule could not be located. In  $[(L^3)_2Ag_4](BF_4)_2$  one adamantyl group was found to be disordered about two positions. SAME restraints and EADP constraints were used to model the disorder. An acetonitrile molecule in the latter compound is disordered about two positions and additionally about a 2-fold rotation axis. The occupancy was set to 0.5. Crystals of  $[(H_2L^1)_4Ag_4](PF_6)_8$  are twinned (twin law 100, 0  $\bar{1}$  0, 0 0  $\bar{1}$ ; BASF 0.486(1)). The molecular structure of  $[H_3L^4][H_2L^4](PF_6)_3$  was refined in the space group  $P1$ . Two molecules are present, one of which is deprotonated at the pyrazole nitrogen atom. The overall charge of +3 is well compensated by three  $PF_6^-$  anions. It is also possible to refine the molecular structure of  $[H_3L^4][H_2L^4](PF_6)_3$  in the space group  $P\bar{1}$ . In this case the hydrogen atom at the pyrazole nitrogen atom and the  $PF_6^-$  counterions are disordered. Hence from a chemical point of view it seemed more reasonable to refine the molecular structure in the space group  $P1$ . The correct absolute structure of  $[H_3L^4][H_2L^4](PF_6)_3$  could not be determined reliably. Water and acetonitrile were found

to be disordered in  $[\text{H}_3\text{L}^4][\text{H}_2\text{L}^4](\text{PF}_6)_3$ . The occupancy for both molecules was set to 0.5. Hydrogen atoms bound to the oxygen atom of the water molecule could not be located. Face-indexed absorption corrections were performed numerically with the program X-RED [24].

CCDC 751084 ( $[(\text{L}^1)_2\text{Ag}_4](\text{BF}_4)_2$ ), CCDC 751085 ( $[(\text{L}^3)_2\text{Ag}_4](\text{BF}_4)_2$ ), CCDC 751086 ( $[(\text{L}^4)_2\text{Ag}_4](\text{PF}_6)_2$ ), CCDC 751087 ( $[(\text{H}_2\text{L}^1)_2\text{Ag}_4](\text{PF}_6)_8$ ), CCDC 751088 ( $[\text{H}_3\text{L}^1](\text{BF}_4)_2$ ), CCDC 751089 ( $[\text{H}_3\text{L}^3](\text{BF}_4)_2$ ), and CCDC 751090 ( $[\text{H}_3\text{L}^4][\text{H}_2\text{L}^4](\text{PF}_6)_3$ ) contain the supplementary crystallographic data for this paper. These data can be obtained free of charge from The Cambridge Crystallographic Data Centre via [www.ccdc.cam.ac.uk/data\\_request/cif](http://www.ccdc.cam.ac.uk/data_request/cif).

#### Supporting Information

ORTEP plots of the molecular structures and selected structural parameters of  $[\text{H}_3\text{L}^1](\text{BF}_4)_2$ ,  $[\text{H}_3\text{L}^3](\text{BF}_4)_2$ , and  $[\text{H}_3\text{L}^4](\text{PF}_6)_2$  are available online (Figs. S1, S2, and S3).

#### Acknowledgements

We thank the Fonds der Chemischen Industrie for financial support. We also would like to thank the groups of Prof. U. Diederichsen and Prof. C. Steinem (University of Göttingen) for measurement of fluorescence spectra.

- [1] a) P.L. Arnold, I.J. Casely, *Chem. Rev.* **2009**, *109*, 3599–3611; b) K.R. Jain, W.A. Herrmann, F.E. Kühn, *Curr. Org. Chem.* **2008**, *12*, 1468–1478; c) N. Marion, S.P. Nolan, *Acc. Chem. Res.* **2008**, *41*, 1440–1449; d) H. Clavier, S.P. Nolan, *Ann. Rep. Progr. Chem. B (Org. Chem.)* **2007**, *103*, 193–222.
- [2] H.M.J. Wang, I.J.B. Lin, *Organometallics* **1998**, *17*, 972–975.
- [3] J.C. Garrison, W.J. Youngs, *Chem. Rev.* **2005**, *105*, 3978–4008.
- [4] I.J.B. Lin, C.S. Vasam, *Coord. Chem. Rev.* **2007**, *251*, 642–670.
- [5] J.C.Y. Lin, R.T.W. Huang, C.S. Lee, A. Bhattacharyya, W.S. Hwang, I.J.B. Lin, *Chem. Rev.* **2009**, *109*, 3561–3598.
- [6] a) E. Peris, R.H. Crabtree, *Coord. Chem. Rev.* **2004**, *248*, 2239–2246; b) O. Köhl, *Chem. Soc. Rev.* **2007**, *36*, 592–607.
- [7] S.-J. Jeon, R.M. Waymouth, *Dalton Trans.* **2008**, 437–439.
- [8] U.J. Scheele, M. John, S. Dechert, F. Meyer, *Eur. J. Inorg. Chem.* **2008**, 373–377.
- [9] Y. Zhou, W. Chen, *Organometallics* **2007**, *26*, 2742–2746.
- [10] U.J. Scheele, M. Georgiou, M. John, S. Dechert, F. Meyer, *Organometallics* **2008**, *27*, 5146–5151.
- [11] a) H.H. Murray, R.G. Raptis, J.P. Fackler, Jr., *Inorg. Chem.* **1988**, *27*, 26–33; b) H.V.R. Dias, H.V.K. Diyabalanage, *Polyhedron* **2006**, *25*, 1655–1661; c) D.M.M. Krishantha, C.S.P. Gamage, Z.A. Schelly, H.V.R. Dias, *Inorg. Chem.* **2008**, *47*, 7065–7067; d) F. Meyer, A. Jacobi, L. Zsolnai, *Chem. Ber./Recueil* **1997**, *130*, 1441–1447.
- [12] a) C. Foces-Foces, I. Alkorta, J. Elguero, *Acta Crystallogr.* **2000**, *B56*, 1018–1028; b) A. Sachse, L. Penkova, G. Nöel, S. Dechert, O.A. Varzatskii, I.O. Fritsky, F. Meyer, *Synthesis* **2008**, *5*, 800–806.
- [13] U.J. Scheele, S. Dechert, F. Meyer, *Inorg. Chim. Acta* **2006**, *359*, 4891–4900.
- [14] Y. Zhou, X. Zhang, W. Chen, H. Qiu, *J. Organomet. Chem.* **2008**, *693*, 205–215.
- [15] Selected Reviews: a) P. Pykkö, *Chem. Rev.* **1997**, *97*, 597–636; b) H. Schmidbaur, A. Schier, *Chem. Soc. Rev.* **2008**, *37*, 1931–1951.
- [16] a) M. Jansen, *Angew. Chem.* **1987**, *99*, 1136–1149; *Angew. Chem., Int. Ed. Engl.* **1987**, *26*, 1098–1110; b) C.-M. Che, S.-W. Lai, *Coord. Chem. Rev.* **2005**, *249*, 1296–1309.
- [17] G. Yang, R.G. Raptis, *Inorg. Chim. Acta* **2007**, *360*, 2503–2506.
- [18] The double-crowned type **B** complex was obtained from the ligand precursor 3,5-bis[3-(2,6-diisopropylphenyl)imidazolium-1-ylmethyl]-1*H*-pyrazole bis(hexafluorophosphate).
- [19] A. Bax, R.H. Griffey, B.L. Hawkins, *J. Magn. Reson.* **1983**, *55*, 301–315.
- [20] R.K. Harris, E.D. Becker, S.M. Cabral de Menezes, R. Goodfellow, P. Granger, *Pure Appl. Chem.* **2001**, *73*, 1795–1818.
- [21] J.C. Röder, F. Meyer, H. Pritzkow, *Organometallics* **2001**, *20*, 811–817.
- [22] M. Stollenz, C. Große, F. Meyer, *Chem. Commun.* **2008**, 1744–1746.
- [23] G.M. Sheldrick, *Acta Cryst.* **2008**, *A64*, 112–122.
- [24] X-RED, Crystal Optimisation for Numerical Absorption Correction, Stoe & Cie GmbH, Darmstadt (Germany) **2002**.

# Structural Variations in Tetrasilver(I) Complexes of Pyrazolate-Bridged Compartmental *N*-Heterocyclic Carbene Ligands

Maria Georgiou, Simone Wöckel, Vera Konstanzer, Sebastian Dechert, Michael John, and Franc Meyer\*

Institut für Anorganische Chemie, Georg-August-Universität Göttingen, Tammannstrasse 4  
D-37077 Göttingen, Germany

## Supporting Information

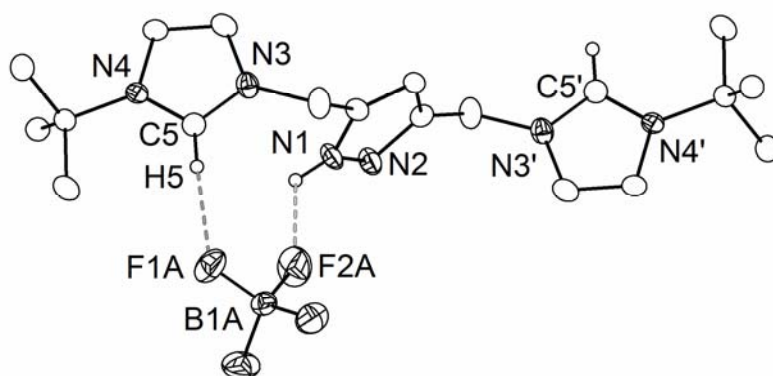


Fig. S1. ORTEP plot (30 % probability displacement ellipsoids) of the molecular structure of  $[\text{H}_3\text{L}^1](\text{BF}_4)_2$  emphasizing the hydrogen bonding interactions. For the sake of clarity most hydrogen atoms and one of the  $\text{BF}_4^-$  ions have been omitted. Symmetry transformations used to generate equivalent atoms: (')  $1-x, 1-y, 2-z$ . Selected parameters for hydrogen bonding or close contacts (Å; deg):  $\text{C5}\cdots\text{F1A/B}$  3.278(3)/3.02(2),  $\text{N1}\cdots\text{F2A}$  3.315(5);  $\text{C5-H5}\cdots\text{F1A/B}$  166(3)/148(3),  $\text{N1-H1}\cdots\text{F2A}$  118.

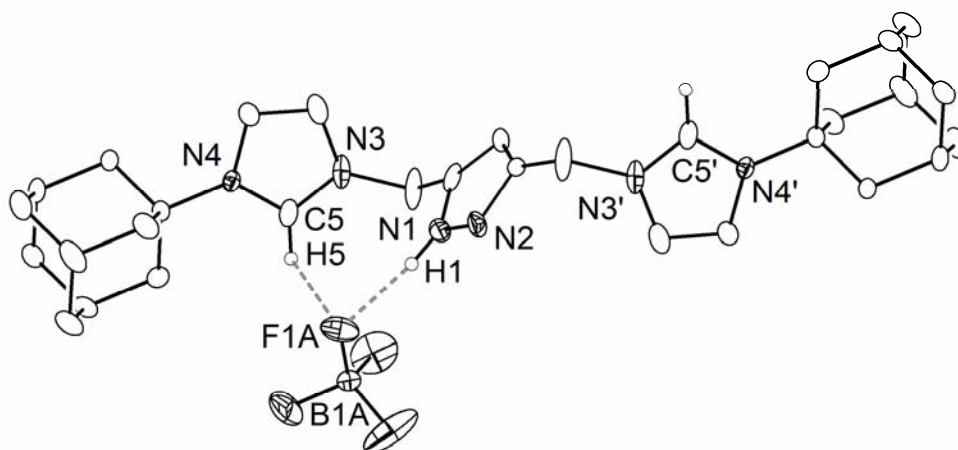


Fig. S2. ORTEP plot (30 % probability displacement ellipsoids) of the molecular structure of  $[\text{H}_3\text{L}^3](\text{BF}_4)_2$  emphasizing the hydrogen bonding interactions. For the sake of clarity most hydrogen atoms and one of the  $\text{BF}_4^-$  ions have been omitted. Symmetry transformations used to generate equivalent atoms: (')  $1-x, 1-y, 1-z$ . Selected parameters for hydrogen bonding or close contacts (Å; deg): C5...F1A/F2A 3.06(1)/3.19(2), N1...F1A/B 2.76(1)/2.38(2); C5–H5...F1A/F2A 105/138, N1–H1...F1A/B 171/159.

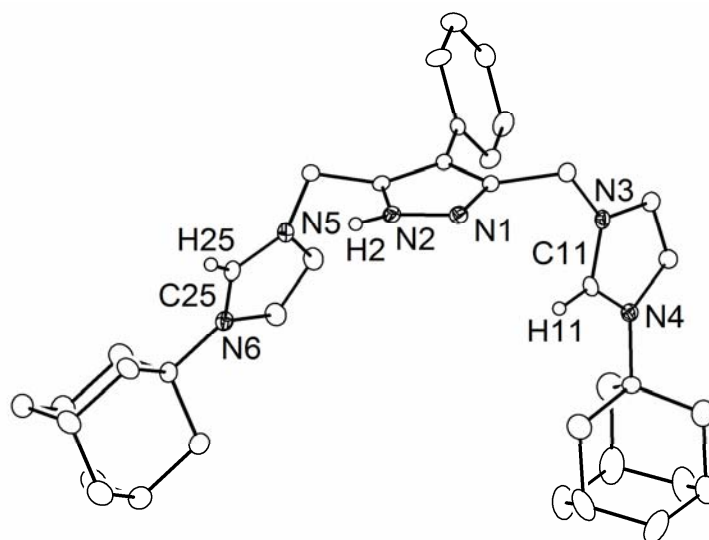


Fig. S3. ORTEP plot (30 % probability displacement ellipsoids) of the molecular structure of the  $[\text{H}_3\text{L}^4]^{2+}$  part of  $[\text{H}_3\text{L}^4][\text{H}_2\text{L}^4](\text{PF}_6)_3$ . For the sake of clarity most hydrogen atoms have been omitted.